Backscatter then Forward: A Relaying Scheme for Batteryless IoT Networks

Bin Lyu, Dinh Thai Hoang, and Zhenzhen Yang

***Abstract*—In this paper, we introduce a novel relaying scheme together with a joint energy beamforming (EB) and time allocation optimization to meet requirements about energy efficiency and hardware constraints of batteryless IoT networks. First, we propose an intelligent relaying scheme using RF-powered gateways as relay nodes to deliver information from batteryless IoT devices to a hybrid access point (HAP). The HAP can also transfer energy to the gateways and batteryless devices using EB techniques. The energy from HAP will be then used to supply power for gateways and as a communications means to transmit data for batteryless devices. We then formulate a sum-rate maximization problem by jointly optimizing the EB vectors, time scheduling, and power allocation. Since the optimization problem is non-convex, we exploit EB characteristics for data backscattering and employ variable substitutions and semidefinite relaxation techniques to transform it into a convex one. After that, a low-complexity method is proposed to obtain the optimal solution in a closed-form. Simulation results confirm that the proposed scheme can achieve significant sum-rate gain.**

***Index Terms*—Wireless power transfer, backscatter communication, relay transmission, energy beamforming.**

I. Introduction

With the development of Internet-of-Things (IoT), wireless devices have been deployed ubiquitously. However, the lifetimes of wireless devices are limited since they are mostly powered by their embedded energy sources, which is one of the main challenges for the pervasive development of IoT. Thus, batteryless IoT communications have been emerging recently as a promising solution to address this issue. In a batteryless IoT communication system, IoT devices transmit data passively by reflecting the instantaneous incident signals from the RF sources based on the backscatter communication (BackCom) technology [1]-[3]. However, as shown in [1], [2], batteryless IoT devices are only appropriate for short-range communications, e.g., in power-constrained wireless sensor networks (WSNs). Hence, solutions to enhance communication ranges for batteryless IoT networks are urgent needs.

Relaying has been well known to be an effective scheme to enhance communication ranges for power-constrained IoT networks. Recently, the BackCom devices operating as relay nodes have been considered [4]-[6]. In [4], a BackCom device was employed as a relay node, which backscatters the received signals from the source node to the destination node to improve signal diversity. To further enhance network performance, [5] employed multiple BackCom devices to work cooperatively for data forwarding (DF), where the joint design of reflection coefficients for BackCom devices is investigated. However, the main limitation of [4] and [5] is that BackCom devices have limited communication ranges, and thus this solution cannot meet the requirement of network coverage, which is especially important for relay networks. In [6], a multi-hop relaying scheme to extend the network coverage was proposed. However, since each-hop relaying by BackCom devices relies on the incident signals from the RF source, it is not energy-efficient for IoT networks. Moreover, the distance between two adjacent BackCom devices should be carefully designed to enable DF, which may be intractable in practice. In [7] and [8], the relay nodes equipped with energy harvesting (EH) circuits and BackCom circuits were used for DF in IoT networks, which aims to exploit the advantages of both active RF communication and BackCom. However, in practice, dual mode devices require more complex integration circuits for switching modes and consume much more power [5], and thus it might not be appropriate to implement widely in power-constrained IoT networks. More importantly, the ceiling of these relays' communication ranges is still limited by the BackCom mode. As mentioned, wireless devices are expected to be batteryless in the future IoT networks, and thus it places some challenges (e.g., extending network coverage with higher energy efficiency), and thus a more efficient relaying scheme for batteryless IoT networks should be addressed.

In this paper, we first propose an energy-efficient backscatter-then-forward framework for batteryless IoT networks, where wireless-powered gateways are used as relay nodes to receive and deliver information from batteryless devices to the HAP. In this framework, the data decoding and forwarding processes are both uploaded to the gateways, which enables the implementation of hardware-constrained batteryless devices for IoT networks. Different from the BackCom relay nodes considered in [4]-[6], the gateways can be randomly deployed around the batteryless devices but significantly extend network coverage. Compared with the hybrid relaying schemes in [7] and [8], the gateways are more appropriate for power-constrained IoT networks and can avoid the limitation of DF distances caused by BackCom. In addition, the gateways can harvest sustainable energy from the HAP and are thus free from the lifetime limitation. We further exploit energy beamforming (EB) [9] at the HAP to improve its energy transfer efficiency and thus improve the achievable system rates. As a result, the coverage of batteryless IoT networks can be extended with higher energy and communication efficiency.

We then investigate the joint design of EB vectors, time

B. Lyu and Z. Yang are with Nanjing University of Posts and Telecommunications, Nanjing 210003, China (e-mail: {blyu, yangzz}@njupt.edu.cn).

D. T. Hoang is with University of Technology Sydney, Sydney, NSW 2007, Australia (e-mail: hoang.dinh@uts.edu.au).

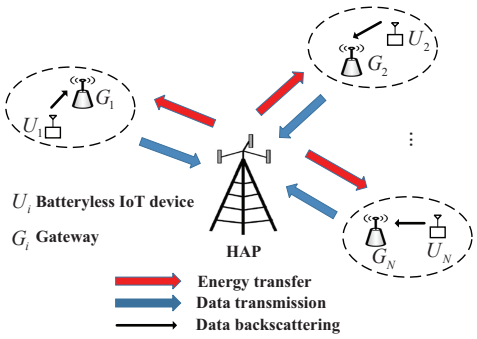

Fig. 1: System model.

scheduling, and power allocation to maximize the system sum-rate. To deal with the non-convex issue of the formulated problem, we first design the EB vectors during the data backscattering (DB) phase by exploiting the characteristics of DB. Then, we employ variable substitutions and semidefinite relaxation (SDR) techniques [10] to transform the non-convex problem into an equivalent convex optimization problem. After that, a low-complexity method is proposed to obtain the optimal solution in the closed-form. The obtained results show the characteristics of the design of EB vectors during the EH phase, and reveal the insights of time scheduling and power allocation.

II. System Model

As shown in Fig. 1, we consider a batteryless IoT network for practical applications, e.g., smart home and logistics [11]. There are N WSNs randomly deployed around an HAP. Each WSN consists of a sensor (batteryless IoT device, denoted by $U_i, i = 1, \ldots, N$) and a gateway (denoted by $G_i, i = 1, \ldots, N$).[1] The HAP with embedded energy sources supplies stable power to all sensors and gateways. The HAP has M antennas and the other devices are all with single antenna. The sensors are hardware-constrained and can only support BackCom circuits for data transmission. The gateways are equipped with EH circuits to support the harvest-then-transmit mode [12], following which they first harvest energy from the HAP and then use the harvested energy for DB. Information decoders are also equipped at the gateways to retrieve the received signals from the sensors due to that the sensors' reflected signals have different power levels [5]. Since the gateway each has only single antenna, they can only either harvest energy or receive and decode backscattered signals at a time. Considering the limited transmission functionality of sensors, the gateways are employed to operate as relay nodes to assist the data transmissions from the senors to the HAP.

A transmission block, normalized to be one, is divided into three phases, i.e., EH phase, DB phase, and DF phase. In the EH phase, all gateways harvest energy from the HAP and store the harvested energy in their batteries, while all sensors keep idle because the gateways can not receive and decode the backscattered signals from the sensors when EH is performed. Denote the transmit signal at the HAP in the first phase as $\boldsymbol{w}(t) = \sqrt{P_H}\hat{\boldsymbol{w}}_0 s(t)$, where $\sqrt{P_H}$ is the transmit power of the HAP, $\hat{\boldsymbol{w}}_0 \in \mathbb{C}^{M\times 1}$ is the EB vector and satisfies $||\hat{\boldsymbol{w}}_0||^2 \leq 1$, $s(t)$ is a known sequence with unit power. The received signal at G_i, denoted by $y_{i,g}(t)$, is expressed as $y_{i,g}(t) = \sqrt{P_H}\boldsymbol{h}_{i,g}^H\hat{\boldsymbol{w}}_0 s(t) + n_{i,g}$, where $\boldsymbol{h}_{i,g} \in \mathbb{C}^{M\times 1}$ is the complex channel vector between the HAP and G_i, and $n_{i,g}$ is the additive white Gaussian noise (AWGN) with zero-mean and variance $\sigma_{i,g}^2$. The harvested energy by G_i, denoted by E_i, is given by $E_i = \eta P_H|\boldsymbol{h}_{i,g}^H\hat{\boldsymbol{w}}_0|^2 b$, where b is the duration of the first phase.

In the DB phase, the sensors utilize the signals from the HAP to backscatter data to the gateways via time division multiple access. Denote the duration of U_i for DB as t_i. The HAP with beamforming aims to focus energy signals to a specified direction during t_i, e.g., U_i, to enhance energy and communication efficiency. Hence, the energy transferred to other sensors is negligible for harvesting. The received signal at U_i, denoted by $u_i(t)$, is expressed as $u_i(t) = \sqrt{P_H}\boldsymbol{h}_{i,u}^H\hat{\boldsymbol{w}}_i s(t) + n_{i,u}$, where $\boldsymbol{h}_{i,u}$ is the complex channel vector between the HAP and U_i, $\hat{\boldsymbol{w}}_i$ is the normalized EB during t_i, and $n_{i,u}$ is the noise at the antenna. The backscattered signal at U_i, denoted by $x_i(t)$, is then given by $x_i(t) = \sqrt{P_H}\boldsymbol{h}_{i,u}^H\hat{\boldsymbol{w}}_i s(t)\alpha_i c_i(t) + n_{i,u}\alpha_i c_i(t)$, where α_i is the reflection coefficient of U_i and satisfies $|\alpha_i|^2 \leq 1$, $c_i(t)$ is U_i's own signal and satisfies $\mathbb{E}[|c(t)|^2] = 1$. Since the sensors operating in the BackCom mode have very limited communication ranges [1], we do not consider the received signals from other sensors at G_i. The received signal at G_i, denoted by $\bar{y}_{i,g}(t)$, is thus formulated as $\bar{y}_{i,g}(t) = \sqrt{P_H}g_{i,u}\boldsymbol{h}_{i,u}^H\hat{\boldsymbol{w}}_i s(t)\alpha_i c_i(t) + g_{i,u}n_{i,u}\alpha_i c_i(t) + \sqrt{P_H}\boldsymbol{h}_{i,g}^H\hat{\boldsymbol{w}}_i s(t) + n_{i,g}$, where $g_{i,u}$ is the complex channel variable between U_i and G_i, and $n_{i,g} \sim \mathcal{CN}(0, \sigma_{i,g}^2)$ is the noise at G_i. Note that the power of $g_{i,u}n_{i,u}\alpha_i c_i(t)$ is quite smaller than that of $n_{i,g}$ due to the path-loss and can be negligible. The third term of $\bar{y}_{i,g}(t)$ is the interference from the HAP, the power of which is larger than that of the desired signal and can be removed by the interference cancellation techniques. After interference cancellation, the signal-noise-ratio (SNR) at G_i is formulated as $\gamma_{i,g} = P_H|g_{i,u}|^2|\boldsymbol{h}_{i,u}^H\hat{\boldsymbol{w}}_i|^2|\alpha_i|^2/\sigma_{i,g}^2$.

In the DF phase, the gateways forward the received signals from the sensors to the HAP sequentially. G_i decodes its received signal and forwards its outcome $c_i(t)$ to the HAP during τ_i. Denote the received signal from G_i at the HAP during τ_i as $\boldsymbol{y}_{i,h}(t)$. $\boldsymbol{y}_{i,h}(t)$ is expressed as $\boldsymbol{y}_{i,h}(t) = \sqrt{P_{i,g}}\boldsymbol{g}_{i,g}c(t) + \boldsymbol{n}_h(t)$, where $P_{i,g}$ is the transmit power at G_i and satisfies $P_{i,g}\tau_i \leq E_i$, $\boldsymbol{g}_{i,g}$ is the complex channel vector between G_i and the HAP, and $\boldsymbol{n}_h(t)$ is the AWGN at the HAP, each element of which is with zero-mean and variance σ_h^2. The SNR at the HAP during τ_i is then given by $\gamma_{i,h} = P_{i,g}||\boldsymbol{g}_{i,g}||^2/\sigma_h^2$. Since the decode-and-forward scheme is considered at G_i, the achievable rate from U_i to the HAP, denoted by R_i, is determined by the hop with smaller transmission rate. Hence, R_i is finally formulated as $R_i = \min\{t_i \log_2(1+\gamma_{i,g}), \tau_i \log_2(1+\gamma_{i,h})\}$.

III. Sum-Rate Maximization

In this work, we investigate the system sum-rate maximization problem by jointly optimizing the EB designs, time

[1] This model can be easily extended to the case that each WSN has multiple sensors, but it is beyond the scope of this paper due to the limited space.

scheduling, and power allocation. The constraints for the network are given as follows C1: $R_i \le t_i \log_2(1+\gamma_{i,g})$, C2: $R_i \le \tau_i \log_2(1+\gamma_{i,h})$, C3 : $P_{i,g}\tau_i \le \eta P_H |\boldsymbol{h}_{i,g}^H \hat{\boldsymbol{w}}_0|^2 b$, C4: $b + \sum_{i=1}^N t_i + \sum_{i=1}^N \tau_i \le 1$, and C5: $0 \le b, t_i, \tau_i \le 1, i = 1,\ldots,N$. The optimization problem is given by

$$\max_{b,\boldsymbol{t},\boldsymbol{\tau},\boldsymbol{R},\hat{\boldsymbol{W}},\boldsymbol{P}} \ \sum_{i=1}^N R_i, \quad \text{s.t. C1} - \text{C5}, \tag{P1}$$

where $\boldsymbol{t} = [t_1,\ldots,t_N]$, $\boldsymbol{\tau} = [\tau_1,\ldots,\tau_N]$, $\boldsymbol{R} = [R_1,\ldots,R_N]$, $\hat{\boldsymbol{W}} = [\hat{\boldsymbol{w}}_0, \hat{\boldsymbol{w}}_1,\ldots,\hat{\boldsymbol{w}}_N]$, and $\boldsymbol{P} = [P_{1,g},\ldots,P_{N,g}]$. Note that **P1** is non-convex and difficult to solve directly due to the couples of EB vectors and time variables. Hence, in the following, we introduce a low-complexity method to obtain the optimal solution for **P1** in a closed-form. First, we propose a solution to transform **P1** into a convex optimization problem. In particular, the following lemma is hold.

Lemma 1. *The optimal EB vector during t_i is $\boldsymbol{h}_{i,u}/||\boldsymbol{h}_{i,u}||$, $\forall i$.*

Proof. Please see Appendix A. □

Then, we can transform **P1** into a convex optimization problem by applying the variable substitutions and SDR techniques [10]. We first introduce some auxiliary variables for substitutions. Let $\boldsymbol{W}_0 = \hat{\boldsymbol{w}}_0 \hat{\boldsymbol{w}}_0^H b$ and $e_i = P_{i,g}\tau_i, i = 1,\ldots,N$. Based on Lemma 1 and the auxiliary variables, the constraints C1-C3 are rewritten as C6: $R_i \le t_i \log_2(1 + P_H |g_{i,u}|^2 ||\boldsymbol{h}_{i,u}||^2 |\alpha_i|^2/\sigma_{i,g}^2)$, C7: $R_i \le \tau_i \log_2(1 + e_i ||\boldsymbol{g}_{i,g}||^2/(\sigma_h^2\tau_i))$, and C8: $0 \le e_i \le \eta P_H \text{Tr}(\boldsymbol{h}_{i,g}\boldsymbol{h}_{i,g}^H \boldsymbol{W}_0)$. To guarantee that introducing the auxiliary variable $\boldsymbol{W}_0$ does not violate the constraints of **P1**, we add the following new constraints C9: $\text{Tr}(\boldsymbol{W}_0) \le b$, C10: $\boldsymbol{W}_0 \succeq 0$, and C11: $\text{rank}(\boldsymbol{W}_0) = 1$. With these new constraints, **P1** is reformulated as

$$\max_{b,\boldsymbol{t},\boldsymbol{\tau},\boldsymbol{R},\boldsymbol{W}_0,\boldsymbol{e}} \ \sum_{i=1}^N R_i, \quad \text{s.t. C4} - \text{C11}, \tag{P2}$$

where $\boldsymbol{e} = [e_1,\ldots,e_N]$. Note that **P2** is still non-convex due to the rank-one constraint given in C11. However, interestingly, the SDR technique can be applied to relax the rank-one constraint such that **P2** can be transformed into a convex optimization problem [10]. Moreover, we can easily prove that $t_i \log_2(1 + P_H |g_{i,u}|^2 ||\boldsymbol{h}_{i,u}||^2 |\alpha_i|^2/\sigma_{i,g}^2) = \tau_i \log_2(1 + e_i ||\boldsymbol{g}_{i,g}||^2/(\sigma_h^2\tau_i))$ in the optimal condition. Following this condition, the objective function of **P2** can be formulated as $\sum_{i=1}^N \tau_i \log_2(1 + e_i ||\boldsymbol{g}_{i,g}||^2/(\sigma_h^2\tau_i))$ directly. In addition, C4 is recast as C12: $b + \sum_{i=1}^N \frac{1}{\bar{R}_i}\tau_i \log_2(1 + e_i ||\boldsymbol{g}_{i,g}||^2/(\sigma_h^2\tau_i)) + \sum_{i=1}^N \tau_i \le 1$, where $\bar{R}_i = \log_2(1 + P_H |g_{i,u}|^2 ||\boldsymbol{h}_{i,u}||^2 |\alpha_i|^2/\sigma_{i,g}^2)$. Then, by removing C11 following SDR, **P2** is reformulated as

$$\begin{aligned} \max_{b,\boldsymbol{\tau},\boldsymbol{W}_0,\boldsymbol{e}} \ & \sum_{i=1}^N \tau_i \log_2(1 + e_i ||\boldsymbol{g}_{i,g}||^2/(\sigma_h^2\tau_i)) \\ \text{s.t.} \ & \text{C8, C9, C10, C12, } 0 \le b \le 1, 0 \le \tau_i \le 1 - b, \forall i. \end{aligned} \tag{P3}$$

It can be proved that the objective function is concave following the perspective operation [13]. Similarly, C12 is convex. In addition, other constraints are all affine. Hence, **P3** is a convex optimization problem.

To solve **P3** efficiently and show the insights about EB design and resource allocation, we propose a two-stage method. First, we solve **P3** with a given b. Then, we update b with the one-dimensional search method. With a given b, **P3** is simplified as follows

$$\begin{aligned} R_{\text{sum}}(b) = \max_{\boldsymbol{\tau},\boldsymbol{W}_0,\boldsymbol{e}} \ & \sum_{i=1}^N \tau_i \log_2(1 + e_i ||\boldsymbol{g}_{i,g}||^2/(\sigma_h^2\tau_i)) \\ \text{s.t.} \ & \text{C8, C9, C10, C12, } 0 \le \tau_i \le 1 - b, \forall i. \end{aligned} \tag{P4}$$

P4 can be solved efficiently by Lagrange duality method, the Lagrangian of which is formulated as $\mathcal{L}(\boldsymbol{\tau}, \boldsymbol{e}, \boldsymbol{W}_0, \mu_i, \rho, \zeta) = \sum_{i=1}^N (1 - \frac{\zeta}{\bar{R}_i})\tau_i \log_2(1 + e_i ||\boldsymbol{g}_{i,g}||^2/(\sigma_h^2\tau_i)) - \sum_{i=1}^N \mu_i e_i + \rho b - \zeta b + \zeta - \zeta \sum_{i=1}^N \tau_i + \text{Tr}(\boldsymbol{V}\boldsymbol{W}_0)$, where $\boldsymbol{V} \triangleq \eta P_H \sum_{i=1}^N \mu_i \boldsymbol{h}_{i,g}\boldsymbol{h}_{i,g}^H - \rho \boldsymbol{I}_M$, $\mu_i \ge 0$, $\rho \ge 0$, and $\zeta \ge 0$ are the Lagrangian multipliers associated with C8, C9, and C12, respectively. Then, the dual function is given by $\mathcal{G}(\mu_i, \rho, \zeta) = \max_{\boldsymbol{W}_0 \succeq 0, e_i \ge 0, 0 \le \tau_i \le 1-b} \mathcal{L}(\boldsymbol{\tau}, \boldsymbol{e}, \boldsymbol{W}_0, \mu_i, \rho, \zeta)$, and the dual problem is expressed as $\min_{\mu_i \ge 0, \rho \ge 0, \zeta \ge 0} \mathcal{G}(\mu_i, \rho, \zeta)$. According to [13], solving **P4** is equivalently to solving its dual problem. Hence, we first achieve $\mathcal{G}(\mu_i, \rho, \zeta)$ with given μ_i, ρ, and ζ, and then minimize $\mathcal{G}(\mu_i, \rho, \zeta)$ by updating μ_i, ρ, and ζ.

Theorem 1. *The optimal solution for **P4** is given by*

$$\boldsymbol{W}_0^* = \boldsymbol{u}_{\boldsymbol{A},1}\boldsymbol{u}_{\boldsymbol{A},1}^H b, \tag{1}$$

$$e_i^* = \eta P_H Tr(\boldsymbol{h}_{i,g}\boldsymbol{h}_{i,g}^H \boldsymbol{W}_0^*), \ i = 1,\ldots,N, \tag{2}$$

$$\tau_i^* = \min\{e_i^* \frac{||\boldsymbol{g}_{i,g}||^2}{\sigma_h^2 z_i^*}, 1 - b\}, \ i = 1,\ldots,N, \tag{3}$$

where $\boldsymbol{u}_{\boldsymbol{A},1}$ is the unit-norm eigenvector of $\boldsymbol{A}$, which corresponds to the maximum eigenvalue $\lambda_{\boldsymbol{A},1}$, $\boldsymbol{A} \triangleq \eta P_H \sum_{i=1}^N \mu_i \boldsymbol{h}_{i,g}\boldsymbol{h}_{i,g}^H$, $z_i^* \ge 0$ is the unique solution of $(1 - \frac{\zeta^*}{\bar{R}_i})f(z_i) = \zeta^*$, and $f(z_i) = \log_2(1+z_i) - \frac{z_i}{\ln(2)(1+z_i)}$. In addition, $\mu_i^* > 0, i = 1,\ldots,N$, $\rho^* = \lambda_{\boldsymbol{A},1}$, and $\zeta^* \le \bar{R}_i$.

Proof. Please see Appendix B. □

It is obvious that $\boldsymbol{W}_0^*$ shown in (1) is a rank-one matrix, which implies that applying SDR in **P2** will not affect the optimal EB design. In other words, the optimal solution obtained from **P4** is also a solution for **P2** with a given b. Moreover, we can straightforwardly obtain an optimal EB vector in the EH phase from (1), which is given by

$$\hat{\boldsymbol{w}}_0^* = \boldsymbol{u}_{\boldsymbol{A},1}. \tag{4}$$

From (4), we observe that to maximize the amount of harvested energy of sensors, the best way is to *multicast* energy signals to all sensors. From (2) and (3), we observe that all sensors are involved in data transmission and the gateways will use all their harvested energy for DF. The amount of time used for the gateways' DF is mainly determined by $||\boldsymbol{h}_{i,g}||^2 ||\boldsymbol{g}_{i,g}||^2$ and $\bar{R}_i$, i.e., the larger $||\boldsymbol{h}_{i,g}||^2 ||\boldsymbol{g}_{i,g}||^2$ and $\bar{R}_i$ lead to a larger DF time, which coincides with the intuition that more time should be allocated to the WSNs with better channel conditions to maximize the sum-rate.

Then, we aim to update the Lagrange multipliers. Since $\rho^* = \lambda_{\boldsymbol{A},1}$ is obtained in Theorem 1, we only need to update μ_i and ζ via the sub-gradient method [13], which are given by $\mu_i^{(l+1)} = (\mu_i^{(l)} - \beta_i^{(l)}(\eta P_H \text{Tr}(\boldsymbol{h}_{i,g}\boldsymbol{h}_{i,g}^H \boldsymbol{W}_0^*) - e_i^*))^+$, $\zeta^{(l+1)} = \min\{(\zeta^{(l)} - \phi^{(l)}(1 - \sum_{j=1}^N \tau_j^*/\bar{R}_j \log_2(1 + e_j^* ||\boldsymbol{g}_{j,u}||^2/(\sigma_h^2\tau_j^*)) -$

$b - \sum_{j=1}^{N} \tau_j^*))^+, \bar{R}_i\}$, where $\beta_i^{(l)}$ and $\phi^{(l)}$ are the step sizes at the lth iteration, and $(x)^+ = \max\{0, x\}$. An algorithm to solve **P4** is summarized in Algorithm 1. As shown in Algorithm 1, we first obtain the optimal solution shown in Theorem 1 with the given Lagrange multipliers (i.e., steps 3-4), and then update the Lagrange multipliers by the sub-gradient method (i.e., step 5). After iterations of the above steps (i.e., steps 3-5), we can obtain the optimal solution $\boldsymbol{W}_0^*$, e_i^*, and τ_i^* at the optimal Lagrange multipliers μ_i^* and ζ^*. After that, the optimal power allocation $P_{i,g}^*$ and the optimal time for DB t_i^* are computed in step 7. The computational complexity of Algorithm 1 is analyzed as follows. The complexity of step 3 is $O(N)$, while that of step 4 is $O(1)$. Since the sub-gradient method is used, the complexity of step 5 is $O(N)$ [13]. Hence, the overall complexity of Algorithm 1 is $O(N)$.

Algorithm 1 The Algorithm for Solving **P4**.

1: Initialize: $\mu_i \geq 0$, $0 \leq \zeta \leq \bar{R}_i$.
2: **repeat**
3: Compute e_i^* and τ_i^* by (2) and (3), respectively.
4: Compute $\boldsymbol{W}_0^*$ by (1), and then compute $\hat{\boldsymbol{w}}_0^*$ by (4).
5: Update μ_i and ζ by the sub-gradient method.
6: **until** μ_i and ζ converge.
7: Set $P_{i,g}^* = e_i^*/\tau_i^*$ and $t_i^* = \tau_i^* \log_2(1 + P_{i,g}^* ||\boldsymbol{g}_{i,g}||^2/\sigma_h^2)/\bar{R}_i$.

Based on Algorithm 1, we can obtain the optimal EB vector for EH, time and power allocations with a given b. We then proceed to find the optimal EH time b^* via $b^* = \arg\max_b R_{\text{sum}}(b)$, where $R_{\text{sum}}(b)$ is defined in **P4**. According to [13], $R_{\text{sum}}(b)$ is a concave function with respect to b, which can be efficiently solved by the golden search method (the details of this method can be found in [14]). Finally, b^* can be obtained after $\log_2(1/\epsilon)$ times of iterations, where ϵ is the tolerance. The total computational complexity of solving **P3** is thus $O(N \log_2(1/\epsilon))$. Note that **P3** can also be solved by CVX (http://cvxr.com/cvx/), the worst case computational complexity of which is $O(\max\{M, N\}^4 M^{1/2} \log_2(1/\epsilon))$ [10]. Compared with using CVX, the computational complexity of the proposed method can be significantly reduced.

IV. Simulation Results

In the simulation[2], we consider that all channels follow Rayleigh fading with distribution $\mathcal{CN}(0, d_{m,n}^{-\kappa})$, where $d_{m,n}$ denotes the distance between two devices m and n ($m, n \in \{\text{HAP}, U_i, G_i\}$), κ is the path-loss exponent and is set as 3. Without loss of generality, we assume $d_{U_i,G_i} = 2$ m, $N = 5$, $|\alpha_i|^2 = 1$, $\eta = 0.7$, and $\sigma_{i,g}^2 = \sigma_h^2 = -70$ dBm. The number of antennas at the HAP are set as $M = 5$ and $M = 10$, respectively. The scheme with random EB designs and the scheme with equal time allocation are used as the benchmarks.[3]

Fig. 2(a) shows the effect of the HAP's transmit power on sum-rate with $d_{\text{HAP},G_i} = 9$ m and $d_{\text{HAP},U_i} = 10$ m. It is observed that the sum-rates of all schemes are increasing functions with respect to the transmit power. The proposed scheme under the optimal solution can always achieve a much larger sum-rate than that of the benchmark schemes, and the performance of the scheme with random EB designs is worst. The reason is that DB and DF are both based on the energy from the HAP, and more energy can be transferred to the gateways and the batteryless IoT devices when the optimal EB vectors are designed. Moreover, adding the number of antennas can further enhance the network performance. The reason is that adding the number of antennas leads to a higher diversity, which improves the efficiencies of EH and DB. Fig. 2(b) investigates the sum-rate versus the distance between the HAP and G_i with $P_H = 20$ dBm and $d_{\text{HAP},G_i} + d_{U_i,G_i} = d_{\text{HAP},U_i}$. It can also be found that the sum-rate achieved by the proposed scheme under the optimal solution is largest. As the distance between the HAP and G_i increases, the sum-rates of all schemes reduce. It is due to that the increase of d_{HAP,G_i} reduces the amount of energy harvested by G_i and degrades the data transmission efficiency of the hop between the HAP and G_i. In addition, an important observation is that the descent rates of sum-rates for the proposed scheme and the scheme with equal time allocation versus d_{HAP,G_i} are slower than that of the scheme with random EB designs. The reason is that the optimal EB designs can partially compensate the performance loss caused by the increase of d_{HAP,G_i}.

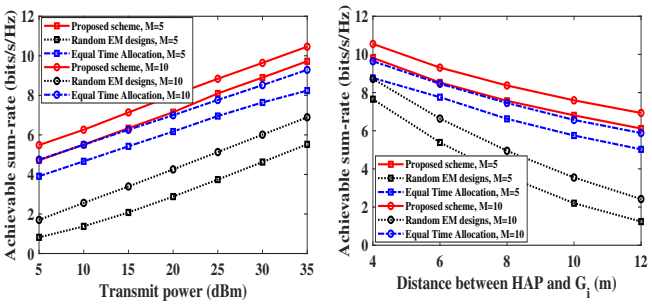

(a) Sum-rate versus P_H. (b) Sum-rate versus d_{HAP,G_i}.

Fig. 2: Performance evaluation.

V. Conclusion

In this paper, we have proposed an intelligent relaying scheme for batteryless IoT networks. The energy-constrained gateways are deployed close to the batteryless devices to assist the communications between them and the HAP. The HAP first beamforms energy signals to the gateways for EH and enables the batteryless devices to backscatter data to their gateways. Then, the gateways use the harvested energy to forward the received signals to the HAP. To maximize the system sum-rate, we have investigated the joint design of EB vectors, time scheduling, and power allocation. Highly effective techniques have been adopted to deal with the non-convex issue of the formulated problem. A two-stage method with low-complexity has been further proposed to find the optimal solution, from which some interesting observations

[2]The simulation codes for our proposed scheme can be downloaded via https://github.com/xinmiwuyou/Backscatter-then-Forward.git.

[3]Similar as the analysis of Algorithm 1, the computational complexities of the benchmark schemes are both $O(N)$.

have been revealed. Simulation results have confirmed the superiority of the proposed scheme.

Appendix A
Proof of Lemma 1

We prove Lemma 1 by contradiction. Denote the optimal energy beamforming vector during t_i as $\hat{\boldsymbol{w}}_i^*$ $(i = 1, \ldots, N)$, where $\hat{\boldsymbol{w}}_i^* \neq \boldsymbol{h}_{i,u}/||\boldsymbol{h}_{i,u}||$. It is easy to obtain that the maximizer of $|\boldsymbol{h}_{i,u}^H \hat{\boldsymbol{w}}_i|^2$ is $\hat{\boldsymbol{w}}_i = \boldsymbol{h}_{i,u}/||\boldsymbol{h}_{i,u}||$. Moreover, $t_i \log_2(1 + P_H|g_{i,u}|^2|\boldsymbol{h}_{i,u}^H \hat{\boldsymbol{w}}_i|^2|\alpha_i|^2/\sigma_{i,g}^2)$ is an increasing function with respect to $|\boldsymbol{h}_{i,u}^H \hat{\boldsymbol{w}}_i|^2$. Hence, R_i^* obtained with $\hat{\boldsymbol{w}}_i = \boldsymbol{h}_{i,u}/||\boldsymbol{h}_{i,u}||$ is not smaller than that obtained with $\hat{\boldsymbol{w}}_i^*$. Hence, $\hat{\boldsymbol{w}}_i^* \neq \boldsymbol{h}_{i,u}/||\boldsymbol{h}_{i,u}||$ is not the optimal solution. This thus proves Lemma 1.

Appendix B
Proof of Theorem 1

The Karush–Kuhn–Tucker (KKT) conditions of **P4** are given as follows [12], [13]

$$\frac{\partial \mathcal{L}}{\partial \tau_i} = (1 - \frac{\zeta^*}{\bar{R}_i}) \log_2(1 + e_i^* ||\boldsymbol{g}_{i,u}||^2/(\sigma_h^2 \tau_i^*)) - (1 - \frac{\zeta^*}{\bar{R}_i}) \frac{e_i^* ||\boldsymbol{g}_{i,u}||^2/(\sigma_h^2 \tau_i^*)}{\ln(2)(1 + e_i^* ||\boldsymbol{g}_{i,u}||^2/(\sigma_h^2 \tau_i^*))} - \zeta^* = 0, \quad (5)$$

$$\mu_i^*(e_i^* - \eta P_H \mathrm{Tr}(\boldsymbol{h}_{i,g} \boldsymbol{h}_{i,g}^H \boldsymbol{W}_0^*)) = 0, \quad (6)$$

$$\boldsymbol{B}\boldsymbol{W}_0^* = 0, \quad (7)$$

$$\rho^*(\mathrm{Tr}(\boldsymbol{W}_0^*) - b) = 0, \quad (8)$$

where $\boldsymbol{B} \triangleq \boldsymbol{A} - \rho^* \boldsymbol{I}_M$, and $\boldsymbol{A} \triangleq \eta P_H \sum_{i=1}^N \mu_i^* \boldsymbol{h}_{i,g} \boldsymbol{h}_{i,g}^H$.

Before we verify (1)-(3) based on the KKT conditions, we first prove $\mu_i^* > 0, i = 1 \ldots, N$ by contradiction. If $\mu_i^* = 0$, there exists a solution that $e_i^* \to \infty$, which leads to $\mathcal{G}(\mu_i, \rho, \zeta) \to \infty$. This contradicts with that $\mathcal{G}(\mu_i, \rho, \zeta)$ is bounded. Hence, we obtain that $\mu_i^* > 0$.

Similarly, we then prove $\rho^* = \lambda_{\boldsymbol{A},1}$, where $\lambda_{\boldsymbol{A},1}$ is the maximum eigenvalue of $\boldsymbol{A}$. Note that $\boldsymbol{B}$ should be a negative semidefinite matrix. The reason is that if $\boldsymbol{B}$ is not negative semidefinite, there exists a solution that $\boldsymbol{W}_0^* = \beta \boldsymbol{\mu}_{\boldsymbol{B}} \boldsymbol{\mu}_{\boldsymbol{B}}^H$ with $\beta \to \infty$, where $\boldsymbol{\mu}_{\boldsymbol{B}}$ is the eigenvector of $\boldsymbol{B}$ corresponding to the positive eigenvalue $\lambda_{\boldsymbol{B}}$, which leads to $\mathcal{G}(\mu_i, \rho, \zeta) \to \infty$. This also contradicts with that $\mathcal{G}(\mu_i, \rho, \zeta)$ is bounded. Hence, $\boldsymbol{B}$ is a negative semidefinite matrix, i.e., $\boldsymbol{B}$ does not have positive eigenvalues. With loss of generality, the eigenvalue decomposition of $\boldsymbol{B}$ can be denoted as $\boldsymbol{B} = \boldsymbol{U}_{\boldsymbol{A}}(\boldsymbol{\Lambda}_{\boldsymbol{A}} - \rho^* \boldsymbol{I}_M)\boldsymbol{U}_{\boldsymbol{A}}$, where $\boldsymbol{U}_{\boldsymbol{A}} \in C^{M \times M}$ is the eigenvector matrix of $\boldsymbol{A}$, and $\boldsymbol{\Lambda}_{\boldsymbol{A}} = \mathrm{diag}(\lambda_{A,1}, \ldots, \lambda_{A,M})$ with $\lambda_{A,1} \geq \ldots \geq \lambda_{A,M}$ is the eigenvalue matrix of $\boldsymbol{A}$. Since $\mu_i^* > 0$, it is obvious that $\boldsymbol{A}$ is a positive semi-definite matrix, i.e., $\lambda_{\boldsymbol{A},i}$, $i = 1, \ldots, N$, is nonnegative. Note that $\lambda_{\boldsymbol{A},1} > 0$ since the rank of $\boldsymbol{A}$ is not smaller than one. Then, to guarantee that the eigenvalues of $\boldsymbol{B}$ are not positive, it is straightforward to obtain that $\rho^* \geq \lambda_{\boldsymbol{A},1} > 0$. Moreover, if $\rho^* > \lambda_{\boldsymbol{A},1}$, $\boldsymbol{B}$ will be a full-rank matrix. Then, to satisfy the constraint given in (7), we have $\boldsymbol{W}_0 = \boldsymbol{0}$, which constricts with the constraint given in (8) due to the fact that $\rho^* > 0$. Hence, we obtain that $\rho^* = \lambda_{\boldsymbol{A},1}$.

Since $\rho^* = \lambda_{\boldsymbol{A},1}$, we have the following observation that the null space of $\boldsymbol{B}$ is spanned by $\boldsymbol{u}_{\boldsymbol{A},1}$, where $\boldsymbol{u}_{\boldsymbol{A},1}$ is the unit-norm eigenvector associated with the maximum eigenvalue $\lambda_{\boldsymbol{A},1}$. According to (7), $\boldsymbol{W}_0$ can be thus expressed as $\boldsymbol{W}_0 = \boldsymbol{u}_{\boldsymbol{A},1} \boldsymbol{u}_{\boldsymbol{A},1}^H \beta$, where $\beta > 0$. Moreover, since $\mathrm{Tr}(\boldsymbol{W}_0) = b$ according to (8), we further have $\beta = b$. Finally, we have $\boldsymbol{W}_0 = \boldsymbol{u}_{\boldsymbol{A},1} \boldsymbol{u}_{\boldsymbol{A},1}^H b$ as given in (1).

We proceed to verify (2) and (3). Since $\mu_i^* > 0$, it is obvious that $e_i^* = \eta P_H \mathrm{Tr}(\boldsymbol{h}_{i,g} \boldsymbol{h}_{i,g}^H \boldsymbol{W}_0^*)$ as shown in (2) according to (6). (5) can be reformulated as

$$(1 - \frac{\zeta^*}{\bar{R}_i}) f(z_i) = \zeta^*, \quad (9)$$

where $f(z_i) = \log_2(1 + z_i) - \frac{z_i}{\ln(2)(1+z_i)}$ and $z_i = e_i^* ||\boldsymbol{g}_{i,g}||^2/(\sigma_h^2 \tau_i^*) \geq 0$. Due to the fact $\zeta^* \geq 0$, to guarantee that there is a solution $z_i^* > 0$ satisfying (9), we have $\bar{R}_i \geq \zeta^*$. Moreover, since $f(z_i)$ is an increasing function with respect to z_i, z_i^* is thus unique. Then, we have $\tau_i^* = e_i^* \frac{||\boldsymbol{g}_{i,g}||^2}{\sigma_h^2 z_i^*} \geq 0$. In addition, $\tau_i^* \leq 1 - b$, we finally obtain τ_i^* as shown in (3).

This thus proves Theorem 1.

References

[1] C. Boyer *et al.*, "Backscatter communication and RFID: Coding, energy, and MIMO analysis," *IEEE Trans. Commun.*, vol. 62, no. 3, pp. 770-785, Mar. 2014.

[2] V. Liu *et al.*, "Ambient backscatter: Wireless communication out of thin air," in *Proc. SIGCOMM*, Hong Kong, Aug. 2013, pp. 39-50.

[3] F. Jameel *et al.*, "Simultaneous harvest-and-transmit ambient backscatter communications under Rayleigh fading," *EURASIP J. Wireless Commun. Netw.*, Dec. 2019.

[4] B. Lyu *et al.*, "User Cooperation in Wireless-Powered Backscatter Communication Networks," *IEEE Wireless Comm. Lett.*, vol. 8, no. 2, pp. 632-635, April 2019.

[5] S. Gong, *et al.*, "Backscatter relay communications powered by wireless energy beamforming," *IEEE Trans. Commun.*, vol. 66, no. 7, pp. 3187-3200, July 2018.

[6] S. H. Kim *et al.*, "Hybrid backscatter communication for wireless-powered heterogeneous networks," *IEEE Trans. Wireless Commun.*, vol. 16, no. 10, pp. 6557-6570, Oct. 2017.

[7] X. Lu *et al.*, "Performance analysis of wireless-powered relaying with ambient backscattering," in *IEEE ICC*, Kansas City, MO, 2018, pp. 1-6.

[8] J. Xu *et al.*, "Passive relaying game for wireless powered Internet of Things in backscatter-aided hybrid radio networks," *IEEE Internet Things J.*, 2019, vol. 6, no. 5, pp. 8933-8944, Oct. 2019.

[9] G. Yang *et al.*, "Multi-antenna wireless energy transfer for backscatter communication systems," *IEEE J. Sel. Areas Commun.*, vol. 33, no. 12, pp. 2974-2987, Dec. 2015.

[10] Z. Q. Luo *et al.*, "Semidefinite relaxation of quadratic optimization problems," *IEEE Signal Process.*, vol. 27, no. 3, pp. 20-34, May 2010.

[11] N. V. Huynh *et al.*, "Ambient backscatter communications: A contemporary survey," *IEEE Commun. Surveys Tuts.*, vol. 20, no. 4, pp. 2889-2922, 4th Quart. 2018.

[12] H. Lee *et al.*, "Sum-rate maximization for multiuser MIMO wireless powered communication networks," *IEEE Trans. Veh. Tech.*, vol. 65, no. 11, pp. 9420-9424, Nov. 2016.

[13] S. Boyd *et. al*, *Convex Optimization*. Cambridge University Press, 2004.

[14] J. Kiefer, "Sequential minimax search for a maximum," *Proc. American Mathematical Society*, vol. 4, no. 3, pp. 502-506, June 1953.